Nucleophilic Addition Reactions of the Osmium−Antimony Cluster (μ-H)Os$_3$(CO)$_9$(μ_3-C$_6$H$_4$)(μ-SbPh$_2$): Orthometalation of Triphenylphosphine at Ambient Temperature

Guizhu Chen, Mingli Deng, Chee Keong Lee, and Weng Kee Leong*

Department of Chemistry, National University of Singapore, Kent Ridge, Singapore 119260

Received November 6, 2001

At ambient temperatures, the reaction of Os$_3$(μ-H)(μ-SbPh$_2$)(μ_3,η^2-C$_6$H$_4$)(CO)$_9$, **1**, with PPh$_3$ proceeded via a nucleophilic addition product, Os$_3$(μ-H)(μ-SbPh$_2$)(μ_2,η^2-C$_6$H$_4$)(CO)$_9$(PPh$_3$), **2a**. This can lose CO to give Os$_3$(μ-H)(μ-SbPh$_2$)(μ_3,η^2-C$_6$H$_4$)(CO)$_8$(PPh$_3$), **3a**, isomerize, deorthometalate to Os$_3$(μ-SbPh$_2$)(C$_6$H$_5$)(CO)$_9$(PPh$_3$), **5a**, or react with excess PPh$_3$ to give an orthometalated product, Os$_3$(μ-SbPh$_2$)(CO)$_8$(PPh$_2$C$_6$H$_4$)(PPh$_3$)$_2$, **6a**. The origin of the orthometalated phenyl ring in **6a** has been established via the reaction of a *p*-tolyl analogue of **2a**, viz., Os$_3$(μ-H)(μ-SbPh$_2$)(μ_2,η^2-C$_6$H$_4$)(CO)$_9${(*p*-tolyl)$_3$P}, **2b**, with PPh$_3$.

Introduction

There is an extensive triosmium cluster chemistry associated with μ_3-phenylene ligands. A common method of synthesis is by P−C,[1] As−C,[2] or S−C[3] bond cleavage via thermolysis of clusters containing ligands with P−Ph, As−Ph, or S−Ph units. The mode of coordination of the μ_3-phenylene group to the metal framework often depends on other ligands on the cluster, and the most common is the μ_3,η^2 mode, in which the phenylene acts as a four-electron donor.[4] The reactivity of these clusters has also been investigated and generally results in substitution at the metal core, for example, with phosphines or alkynes.[5] Reactivity involving the phenylene ring has been less well investigated, one rare example being the Friedel−Crafts acylation and alkylation of the phenylene complexes Os$_3$(μ-H)$_2$(CO)$_9$(arylene) (Scheme 1).[6]

We have recently reported that the thermolysis of the cluster Os$_3$(CO)$_{11}$(SbPh$_3$) led initially to Sb−C cleavage to afford the cluster Os$_3$(μ-H)(μ-SbPh$_2$)(μ_3,η^2-C$_6$H$_4$)(CO)$_9$, **1**,[7] and that it displayed interesting reactivity with alkenes and alkynes, including C−C coupling and deorthometalation of the phenylene.[8] We were thus intrigued if it may react in a novel manner even with apparently simple two-electron donor ligands such as phosphines and isocyanides. Herein we would like to report our investigations of the reactivity of **1** with phosphines, particularly triphenylphosphine.

Scheme 1

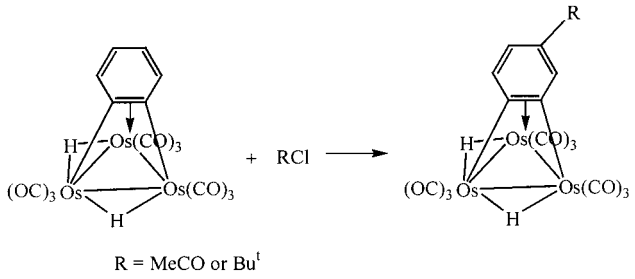

Results and Discussion

The reaction of **1** with excess PPh$_3$ in hexane gave a yellow suspension, from which three bands were obtained after TLC separation. Fractional crystallization of the first band gave yellow crystals of Os$_3$(μ-H)(μ-SbPh$_2$)(μ_3,η^2-C$_6$H$_4$)(CO)$_9$(PPh$_3$), **2a**, and orange crystals of Os$_3$(μ-H)(μ-SbPh$_2$)(μ_3,η^2-C$_6$H$_4$)(CO)$_8$(PPh$_3$), **3a**. Further crystallization of the supernatant afforded crystals of yet another cluster, **4**, which has the same molecular formula as **2a**, but from which a pure sample could not be obtained. All three novel clusters were characterized by single-crystal X-ray crystallographic studies; the ORTEP diagrams showing their molecular structures are given in Figures 1−3, respectively.

The second band from the TLC separation gave a yellow solid in very low yield and hence was not fully characterized. However, the solution IR spectrum in the

(1) (a) Deeming, A. J.; Kabir, S. E.; Powell, N. I.; Bates, P. A.; Hursthouse, M. B. *J. Chem. Soc., Dalton Trans.* **1987**, 1529. (b) Brown, S. C.; Evans, J.; Smart, L. E. *J. Chem. Soc., Chem. Commun*. **1980**, 1021. (c) Deeming, A. J.; Marshall, J. E.; Nuel, D.; O'Brien, G.; Powell, N. I. *J. Organomet. Chem*. **1990**, *384*, 347. (d) Cullen, W. R.; Chacon, S. T.; Bruce, M. I.; Einstein, F. W. B.; Jones, R. H. *Organometallics* **1988**, *7*, 2273. (e) Cullen, W. R.; Rettig, S. T.; Zhang, H. *Organometallics* **1991**, *10*, 2965. (f) Cullen, W. R.; Rettig, S. T.; Zhang, H. *Organometallics* **1992**, *11*, 928. (g) Cullen, W. R.; Rettig, S. T.; Zhang, H. *Organometallics* **1992**, *11*, 1000.

(2) (a) Arce, A. J.; Deeming, A. J. *J. Chem., Soc., Dalton Trans.* **1982**, 1155. (b) Cullen, W. R.; Rettig, S. T.; Zhang, H. *Organometallics* **1993**, *12*, 1964. (c) Johnson, B. F. G.; Lewis, J.; Massey, A. D.; Braga, D.; Grepioni, F. *J. Organomet. Chem*. **1983**, *251*, 261. (d) Jackson, P. A.; et al. *J. Organomet. Chem*. **1990**, *391*, 225.

(3) Adams, R. D.; Katahira, D. A.; Yang, L. W. *Organometallics* **1982**, *1*, 235.

(4) Johnson, B. F. G.; Lewis, J.; Whitton, A. J.; Bott, S. J. *J. Organomet. Chem*. **1990**, *389*, 129.

(5) (a) Chen, H.; Johnson, B. F. G.; Lewis, J.; Raithby, P. R. *J. Organomet. Chem*. **1991**, *406*, 219. (b) Chen, H.; Johnson, B. F. G.; Lewis, J.; Raithby, P. R. *J. Organomet. Chem*. **1991**, *376*, C7.

(6) Chen, H.; Johnson, B. F. G.; Lewis, J. *Organometallics* **1989**, *8*, 2965.

(7) Leong, W. K.; Chen, G. *Organometallics* **2001**, *20*, 2280.

(8) (a) Deng, M.; Leong, W. K. *Organometallics*, in press. (b) Deng, M.; Leong, W. K. *J. Chem. Soc., Dalton Trans*., in press.

10.1021/om010959a CCC: $22.00
Publication on Web 02/20/2002

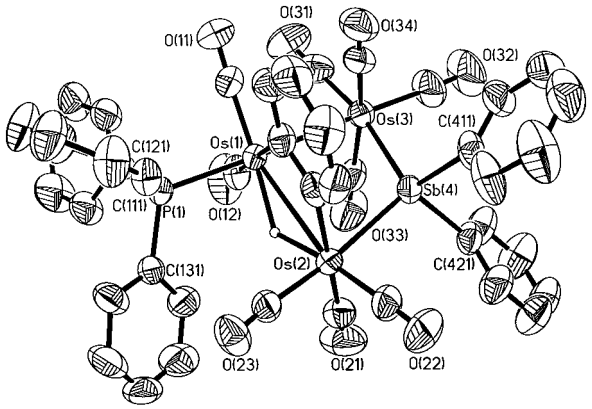

Figure 1. ORTEP diagram (organic hydrogens omitted, 50% probability thermal ellipsoids) for **2a**.

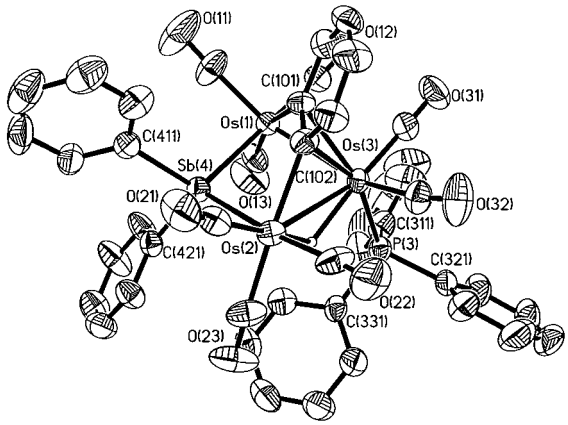

Figure 2. ORTEP diagram (organic hydrogens omitted, 50% probability thermal ellipsoids) for **3a**.

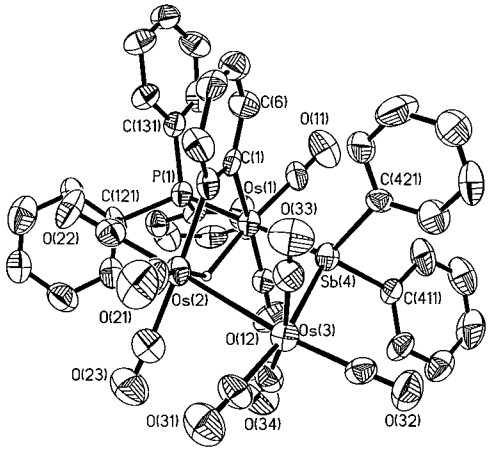

Figure 3. ORTEP diagram (organic hydrogens omitted, 50% probability thermal ellipsoids) for **4**.

carbonyl region of this product was similar to that of $Os_3(\mu\text{-}SbPh_2)(Ph)(CO)_9(PMe_2Ph)$, **5c**, which was obtained from the analogous reaction of **1** with PMe_2Ph. Thus the compound was assigned as $Os_3(\mu\text{-}SbPh_2)(Ph)(CO)_9(PPh_3)$, **5a**; the ORTEP diagram showing the molecular structure of **5c** is given in Figure 4, together with selected bond parameters. The reaction with PMe_2Ph also afforded analogues of **2a** and **3a**, viz., $Os_3(\mu\text{-}H)(\mu\text{-}SbPh_2)(\mu_2,\eta^2\text{-}C_6H_4)(CO)_9(PMe_2Ph)$, **2c**, and $Os_3(\mu\text{-}H)(\mu\text{-}SbPh_2)(\mu_3,\eta^2\text{-}C_6H_4)(CO)_8(PMe_2Ph)$, **3c**.

The third TLC band afforded a yellow solid, which was identified as the novel cluster $Os_3(\mu\text{-}SbPh_2)(CO)_8(PPh_2C_6H_4)(PPh_3)_2$, **6a**; the structure was established by a single-crystal X-ray crystallographic study and is shown in Figure 5, together with selected bond parameters. The structure of **6a** comprises an orthometalated triphenylphosphine. This structural feature is not surprising per se as there are a number of examples of such orthometalation of arylphosphines known. However, the formation of **6a** is exceptional, as such orthometalation of coordinated arylphosphines by osmium clusters normally occurs only under thermolytic conditions.

That clusters **2a**, **3a**, and **4** were obtained from the same TLC band suggested that they were related via a decomposition process. Indeed, when a $CDCl_3$ solution

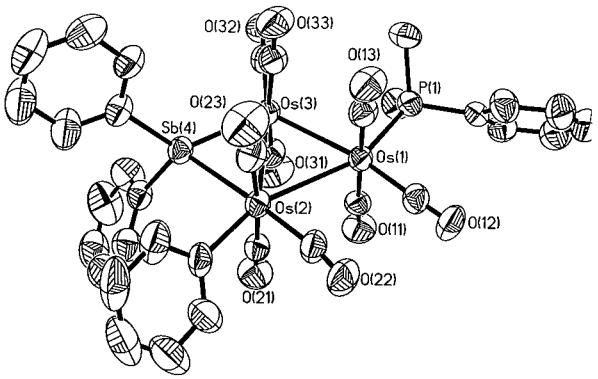

Figure 4. ORTEP diagram (organic hydrogens omitted, 50% probability thermal ellipsoids) and selected bond parameters for **5c**: Os(1)−Os(2) = 3.0018(5) Å; Os(1)−Os(3) = 2.8215(4) Å; Os(2)−Os(3) = 2.9943(5) Å; Os(2)−Sb(4) = 2.6756(6) Å; Os(3)−Sb(7) = 2.5667(6) Å; Os(1)−P(1) = 2.319(2) Å; Os(2)−C(101) = 2.165(9) Å; ∠Os(2)-Os(1)Os(3) = 61.795(11)°; ∠Os(1)Os(2)Os(3) = 56.141(10)°; ∠Os(1)Os(3)Os(2) = 62.064(11)°; ∠Os(2)Sb(4)Os(3) = 69.630(16)°.

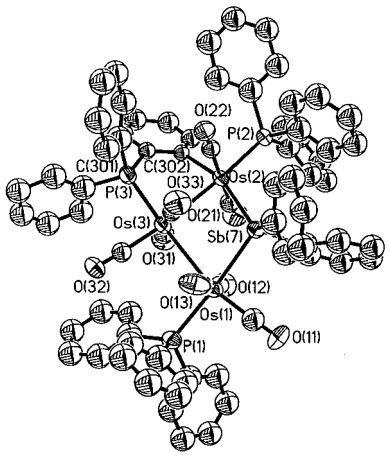

Figure 5. ORTEP diagram for molecule **A** (organic hydrogens omitted, 50% probability thermal ellipsoids) of **6a**. Selected bond parameters, Molecule **A**: Os(1)−Os(3) = 3.0315(10) Å; Os(2)−Os(3) = 2.9648(10) Å; Os(2)−Sb(7) = 2.6720(13) Å; Os(1)−Sb(7) = 2.7051(13) Å; Os(1)−P(1) = 2.429(5) Å; Os(2)−P(2) = 2.318(5) Å; Os(3)−P(3) = 2.331(5) Å; Os(2)−C(302) = 2.157(15) Å; ∠Os(1)Os(3)Os(2) = 92.73(3)°; ∠Os(1)Sb(7)Os(2) = 107.64(4)°. Molecule **B**: Os(4)−Os(6) = 3.0488(9) Å; Os(5)−Os(6) = 2.9749(9) Å; Os(5)−Sb(8) = 2.6597(13) Å; Os(4)−Sb(8) = 2.7011(13) Å; Os(4)−P(4) = 2.416(5) Å; Os(5)−P(5) = 2.328-(5) Å; Os(6)−P(6) = 2.332(4) Å; Os(5)−C(602) = 2.151(16) Å; ∠Os(4)Os(6)Os(5) = 91.96(2)°; ∠Os(4)Sb(8)Os(5) = 107.82(4)°.

Scheme 2

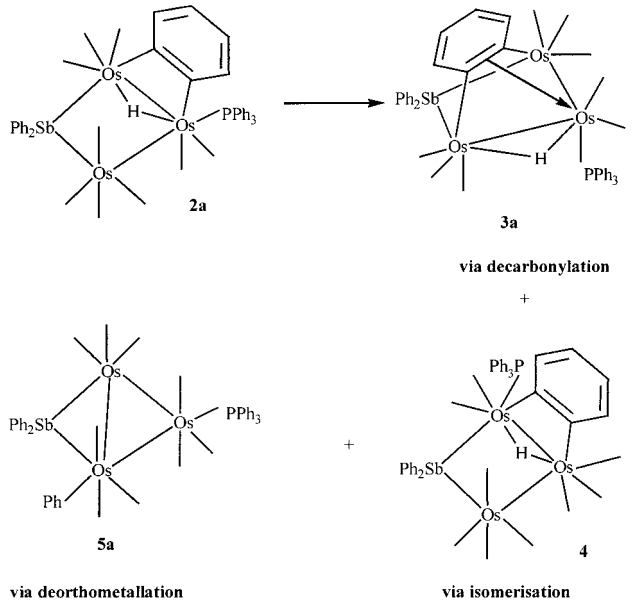

of **2a** was monitored by ^{1}H NMR spectroscopy over several days, the spectrum showed the emergence of two sets of doublets at −16.40 and −18.60 ppm, which was indicative of the formation of **3a** and **4**. Furthermore, the intensities of the latter signals increased at the expense of that for **2a**. A similar monitoring by ^{31}P{^{1}H} NMR spectroscopy also showed the emergence of a very weak resonance ascribable to **5a** after several days of standing, suggesting that **5a** was also derived from **2a**. Scheme 2 shows the possible relationship among these clusters.

Cluster **3a** may be considered as being derived from **2a** by loss of one CO and a change in the bonding mode of the C_6H_4 moiety. By stirring **2a** in a CH_2Cl_2 solution together with silica gel, we have found that the color of the solution changed from yellow to orange gradually, and TLC separation gave cluster **3a** as the only cluster compound present. Furthermore, UV photolysis of a hexane solution of **2a** also gave **3a** in quantitative yield. All these suggested that **2a** should be rather unstable, and indeed it is very difficult to obtain a sample of **2a** that is relatively free of **3a**; a similar situation was observed for the P(*p*-tolyl)$_3$ and PMe_2Ph analogues **2b** and **2c**, respectively.

We have found that the yield of **6a** increased at the expense of that of **2a**. We therefore hypothesized that **6a** was the result of further reaction of **2a** with excess PPh_3. Indeed, **2a** did react with PPh_3 to afford **6a** in high yield after TLC separation. However, when the reaction between **1** and 3 equiv of PPh_3 was monitored by IR and NMR spectroscopy, it was observed that only **2a** was formed directly in the reaction; **6a** was not detected. Thus the ^{1}H NMR spectrum of the reaction mixture showed a singlet at −17.18 ppm (assignable to **1**) and a doublet at −18.41 ppm (assignable to **2a**), but no resonances ascribable to **4**, **3a**, or **6a**. The ^{31}P{^{1}H} NMR spectrum of the reaction mixture showed three sets of resonances at 29.1, 5.4, and −5.2 ppm. The latter two resonances were assignable to **2a** and free PPh_3, respectively. The resonance at 29.1 ppm was therefore assigned to an intermediate, **A**. However, this intermediate was not observed among the products separated

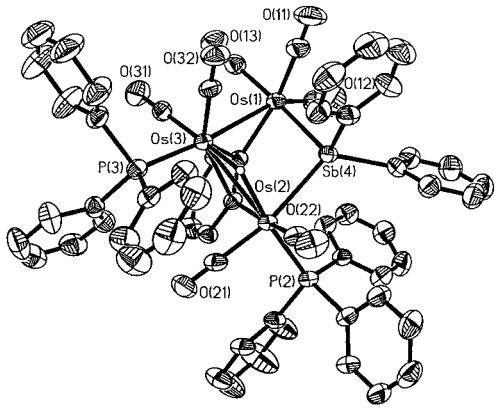

Figure 6. ORTEP diagram (organic hydrogens omitted, 50% probability thermal ellipsoids) and selected bond parameters for **7**.

by TLC; **6a** was obtained in high yield instead. This suggested that **6a** was formed from the decomposition of the intermediate **A** during TLC workup. In contrast, we have also found that cluster **3a** reacted with PPh_3 to give **6a** in quantitative yield. The reaction was monitored by ^{1}H and ^{31}P{^{1}H} NMR spectroscopy; the ^{31}P{^{1}H} NMR spectrum of the reaction mixture showed the presence of an intermediate, **B**, with a resonance at 29.6 ppm. Resonances attributable to **6a** were also found, indicating that **6a** was readily formed from the reaction of **3a** with excess PPh_3, unlike the case for **2a**.

The formation of **6a** from **2a** or **3a** required the accommodation of two additional PPh_3 ligands, loss of the *o*-phenylene, and orthometalation of one of the phenyl rings of a PPh_3. The sequence of these events is not known, and whether the last two events were as described or involved loss of a phenyl from a PPh_3 and coupling of the *o*-phenylene ligand with phosphorus was also uncertain. There was no spectroscopic evidence for any reaction intermediate or product containing two phosphine ligands in the reactions leading to **6a**. We could synthesize a cluster with two phosphine ligands via chemical activation of **1** or **3a** with Me_3NO, viz., $Os_3(\mu\text{-H})_2(\mu\text{-SbPh}_2)(\mu_3,\eta^2\text{-C}_6\text{H}_4)(\text{CO})_7(\text{PPh}_3)_2$, **7**; the ORTEP diagram is given in Figure 6. However, as is readily observed, cluster **7** has seven carbonyl ligands while **6a** has eight. It is therefore unlikely that **7** was an intermediate for the formation of **6a**.

To establish whether the formation of **6a** involved orthometalation or P−C coupling, and also which of the phosphine ligands was orthometalated or dephenylated, $Os_3(\mu\text{-H})(\mu\text{-SbPh}_2)(\mu_3,\eta^2\text{-C}_6\text{H}_4)(\text{CO})_9\{\text{P}(p\text{-tolyl})_3\}$, **2b**, was prepared from the reaction of **1** with P(*p*-tolyl)$_3$; the molecular structure of **2b** has been confirmed by a single-crystal X-ray crystallographic study. Cluster **2b** was then reacted with PPh_3; if the arene that was lost originated from the *o*-phenylene, then orthometalation of a *p*-tolyl group will occur (Scheme 3, route a), and if it is from the P(*p*-tolyl)$_3$, then the orthometalated group will still be an *o*-phenylene (Scheme 3, route b).

The product so obtained was formulated as $Os_3(\mu\text{-SbPh}_2)(\text{CO})_8\{\mu\text{-P}(p\text{-tolyl})_2(\text{C}_6\text{H}_3\text{CH}_3)\}(\text{PPh}_3)_2$, **8**, which was characterized spectroscopically and analytically. The ^{1}H NMR spectrum of **8** exhibited two resonances at 1.73 and 2.39 ppm with a 1:2 relative intensity. These were assignable to CH_3 groups of the *p*-tolyl moiety and indicated that one of the tolyl groups on the P(*p*-tolyl)$_3$

Table 1. Common Atomic Numbering Scheme and Selected Bond Parameters for 2a, 2b, and 4

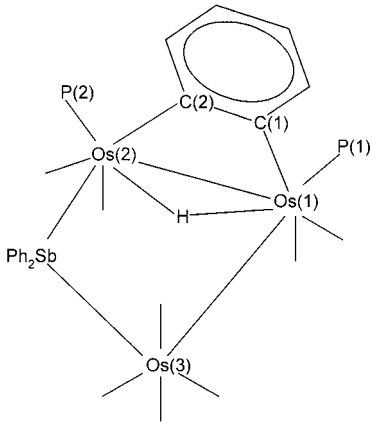

	2a	2b	4
		Bond Lengths (Å)	
Os(1)−Os(2)	3.2332(12)	3.2308(3)	3.2025(8)
Os(1)−Os(3)	3.0298(13)	3.0454(4)	2.9999(8)
Os(2)−Sb	2.6554(15)	2.6706(5)	2.6431(9)
Os(3)−Sb	2.6717(11)	2.6663(5)	2.6773(11)
Os(1)−P(1)	2.365(2)	2.3593(17)	
Os(2)−P(2)			2.382(3)
Os(1)−C(1)	2.159(9)	2.145(6)	2.167(14)
Os(2)−C(2)	2.123(10)	2.133(7)	2.160(13)
C(1)−C(2)	1.437(12)	1.408(9)	1.383(18)
Os−C + C−O	3.02−3.12	3.02−3.09	3.00−3.09
		Bond Angle (deg)	
Os(2)−Os(1)−Os(3)	88.88(3)	88.406(9)	88.75(2)
Os(2)−Sb−Os(3)	110.90(5)	110.228(7)	109.31(4)
Os−C−O	173.3(8)−178.9(10)	171.6(7)−178.3(9)	173.8(14)−179.8(16)

Scheme 3

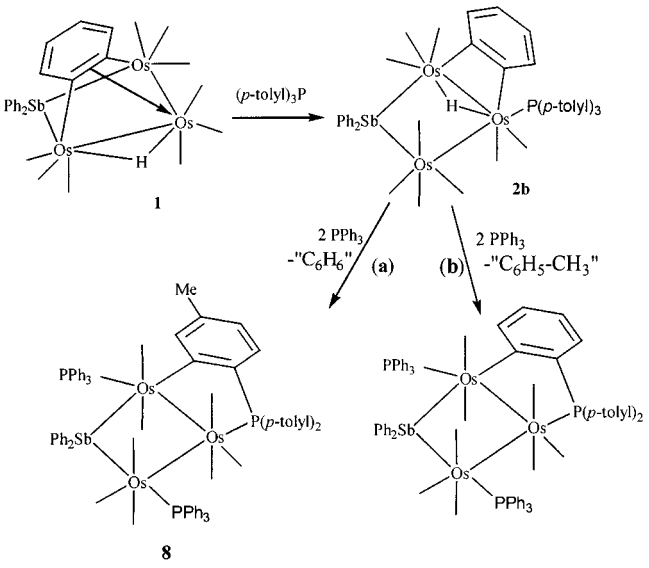

ligand of **2b** has indeed undergone orthometalation, thus supporting pathway a.

Crystallographic Studies

Clusters **2a**, **2b**, and **4** are structurally similar, and **4** is a positional isomer of **2a** differing in the location of the phosphine ligand; selected bond parameters are tabulated in Table 1. These clusters contain an *o*-phenylene ligand, and the clusters are electron-precise if the phenylene is regarded as a two-electron donor. Such a bonding mode has been observed previously only in two dinuclear *o*-phenylene complexes, $Cp_2Ir_2(\mu\text{-}\eta^2\text{-}C_6H_4)(CO)_2$ and $Fe_2(\mu\text{-}\eta^2\text{-}C_6F_4)(CO)_8$,[9] and one trinuclear derivative, $Os_3(\mu\text{-}H)_3(\mu\text{-}\eta^2\text{-}C_6H_4)(CO)_8(HC{=}NC_6H_5)$.[10] The presence of the metal hydride in these clusters is indicated by a doublet at about −18 ppm in the ^{1}H NMR spectrum. The positions of the hydrides were predicted by potential energy calculations, except in **2b**, for which the hydride was located by a low-angle difference map. It is a common observation that the hydride tends to bridge the most electron-rich metal−metal bond, which is that *cis* to the phosphine ligand, even though this is the most sterically hindered metal−metal bond.[11] Both the Os(1)−Os(2) and Os(1)−Os(3) bonds are very long; the latter especially so, exceeding 3.2 Å in the three clusters. This is much longer than the maximum Os−Os bonded distance of 3.05 Å proposed by Deeming,[12] and they are the longest Os−Os bond lengths reported to date. This is probably a combination of the lengthening due to a hydride bridge, further enhanced by the geometrical constraints of an η^2-phenylene, and coordination of a phosphine ligand *cis* to the Os−Os bond.

Selected bond parameters for the clusters **3a**, **3c**, and **7** are given in Table 2. These clusters contain the μ_3,η^2-C_6H_4 ligand, and unlike those above, the Os−Os bond lengths are more typical. The presence of the metal

(9) (a) Rausch, M. D.; Gastinger, R. G.; Gardner, S. A.; Brown, R. K.; Wood, J. S. *J. Am. Chem. Soc.* **1977**, *99*, 7870. (b) Bernett, M. J.; Graham, W. A. G.; Stewart, R. P; Tuggle, R. M. *Inorg. Chem.* **1973**, *12*, 2944.

(10) Adams, R. D.; Golembeski, N. M. *J. Organomet. Chem.* **1979**, *172*, 239.

(11) (a) Churchill, M. R.; Lashewycz, R. A. *Inorg. Chem.* **1978**, *17*, 1950. (b) Adams, R. D.; Golembeski, N. M.; Selegue, J. P. *J. Am. Chem. Soc.* **1981**, *103*, 546.

(12) Deeming, A. J. *Adv. Organomet. Chem.* **1986**, *26*, 6.

Table 2. Common Atomic Numbering Scheme and Selected Bond Parameters for 3a, 3c, and 7

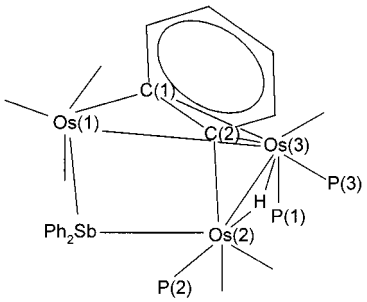

	3a	3c	7
		Bond Lengths (Å)	
Os(1)−Os(3)	2.9065(4)	2.8871(3)	2.8706(3)
Os(2)−Os(3)	2.9626(4)	3.0014(4)	3.0152(3)
Os(1)−Sb	2.6496(6)	2.6403(5)	2.6545(4)
Os(2)−Sb	2.6565(6)	2.6574(5)	2.6763(4)
Os(3)−P(1)	2.3566(19)	2.3194(17)	
Os(2)−P(2)			2.3817(13)
Os(3)−P(3)			2.3896(15)
Os(1)−C(1)	2.165(7)	2.168(6)	2.149(5)
Os(2)−C(2)	2.176(8)	2.187(7)	2.197(5)
Os(3)−C(1)	2.333(8)	2.350(6)	2.366(5)
Os(3)−C(2)	2.342(7)	2.339(6)	2.365(5)
C(1)−C(2)	1.448(10)	1.451(9)	1.446(7)
Os−C + C−O	3.03−3.08	3.05−3.08	3.02−3.08
		Bond Angles (deg)	
Os(1)−Os(3)−Os(2)	87.502(11)	87.576(9)	87.547(8)
Os(1)−Sb−Os(2)	99.806(18)	100.586(16)	99.652(13)
Os−C−O	170.8(9)−177.0(9)	175.4(8)−178.6(7)	175.4(6)−179.0(5)

hydrides is indicated by doublets in the −16 ppm region of their ^{1}H NMR spectra, and potential energy calculations suggested that they bridge the longer Os−Os bonds. The Os−C bond lengths associated with the phenylene ligand are similar to those in the μ,η^2 cases above. However, it is noteworthy that the C(1)−C(2) lengths are generally longer in the μ_3,η^2-C_6H_4 ligands than in the μ,η^2-C_6H_4 ligands; ranges are 1.446(7)−1.451(9) and 1.383(18)−1.437(12) Å, respectively. These values can be compared to the 1.40 Å in benzene[13] and may be indicative of a greater loss of aromaticity in the former ligand bonding mode. The change in the bonding mode from μ,η^2 to μ_3,η^2 is also manifested in the smaller OsOsOs and OsSbOs angles; ∼100° and ∼87.5°, respectively, for the clusters with the μ,η^2 phenylene bonding mode and ∼88° and ∼110°, respectively, for clusters with the μ_3,η^2 bonding mode.

An outstanding structural feature of the clusters **3a** and **3c** is that the phosphine occupies an axial position with respect to the metal framework. There is only one other example of a triosmium cluster with an axially bound phosphorus ligand, viz., $Os_3(\mu\text{-}H)_2(C_4H_3N)(CO)_7[P(OMe)_3]_2$.[5a] The reason for the unusual stereochemistry adopted is not clear, since an axially bound phosphine is not observed for cluster **7**.

Cluster **5** comprises an almost planar Os_3Sb "kite"; the dihedral angle between the Os_3 and Os_2Sb triangular planes is 2.9°. It is the first example of such an Os_3Sb geometry, the closest relation being the Os_3Sb_2 cluster $Os_3(\mu\text{-}SbPh_2)_2(CO)_{10}$ that we have reported earlier.[14] As was also observed in that compound, the Os−Os edge that is bridged by the $SbPh_2$ moiety is somewhat elongated. Contrary to what may be expected, however, the Os−Os bond *cis* to the phosphine ligand is shortest among the Os−Os bonds. Indeed, the Os(1)−Os(2) bond that is *trans* to the phenyl ring is very long at 3.0018(5) Å and suggests that the phenyl competes strongly for π back-donation from the metal. On the other hand, the Os(3)−Sb(4) length at 2.5665(6) Å is the shortest among the simple triosmium−antimony clusters observed to date, possibly to compensate for the steric repulsion between the phenyl ligand on Os(2) and those on Sb(4).

There are two crystallographically distinct molecules in the crystal structure of **6a**. The differences between their bond parameters are mainly those associated with the heavy atoms, the largest being the Os(1)−Os(3) bond lengths, which differ by 18σ. The Os(1)−P(1) bond length is unusually long at ∼2.42 Å and is barely within the sum of the atomic radii for Os and P (2.45 Å).[15] Although the orthometalated phosphine lies more or less in the equatorial plane, it is noticed that the carbonyl ligands on Os(2) are staggered with respect to those on Os(3), adopting what Pomeroy et al. have termed the *S* conformation.[16] In more highly substituted clusters, such as $Os_3(CO)_6[P(OMe)_3]_6$, the *S* geometry is more common. We have earlier suggested that in the monosubstituted triosmium clusters $Os_3(CO)_{11}(PR_3)$ steric effects from the PR_3 ligand led to a propensity toward greater twisting of the $Os(CO)_3(PR_3)$ group.[17] Thus the distortion in cluster **6a** may be attributed to the same

(13) (a) Bastiansen, O.; Fernholt, L.; Seip, H. M.; Kambara, H.; Kuchitsu, K. *J. Mol. Struct.* **1973**, *18*, 163. (b) Tamagawa, K.; Iijima, T.; Kimura, M. *J. Mol. Struct.* **1976**, *30*, 243.

(14) Leong, W. K.; Chen, G. *J. Chem. Soc., Dalton Trans.* **2000**, 4442.

(15) Shriver, D. F.; Atkins, P. W. *Inorganic Chemistry*, 3rd ed.; OUP: Oxford, 1999.

(16) Hansen, V. M.; Ma, A. K.; Biradha, K.; Pomeroy, R. K.; Zaworotko, M. J. *Organometallics* **1998**, *17*, 5267.

(17) Leong, W. K.; Liu, Y. *J. Organomet. Chem.* **1999**, *584*, 5267.

Table 3. Crystal and Refinement Data for 2a, 2b, 3a, 3c, 4, 5c, 6a, and 7

	2a	2b	3a	3c	4	5c	6a	7
empirical formula	$C_{45}H_{30}O_9Os_3PSb$	$C_{48}H_{36}O_9Os_3PSb$	$C_{44}H_{30}O_8Os_3PSb$	$C_{34}H_{26}O_8Os_3PSb$	$C_{45}H_{30}O_9Os_3PSb\cdot CH_2Cl_2$	$C_{35}H_{26}O_9Os_3PSb$	$2C_{74}H_{54}O_8Os_3P_3Sb\cdot 3/4CH_2Cl_2$	$C_{61}H_{45}O_7Os_3P_2Sb\cdot CH_2Cl_2$
fw	1438.01	1480.09	1410.00	1285.87	1522.94	1313.88	3776.56	1729.19
cryst syst	monoclinic	monoclinic	monoclinic	triclinic	triclinic	monoclinic	triclinic	triclinic
space group	$P2_1/c$	$P2_1/n$	$P2_1/c$	$P\bar{1}$	$P\bar{1}$	$P2_1/c$	$P\bar{1}$	$P\bar{1}$
a, Å	13.1280(2)	13.7183(2)	9.7194(2)	10.4650(2)	12.9772(2)	18.6644(1)	13.4047(1)	12.0001(2)
b, Å	18.9541(2)	17.4565(3)	10.7339(3)	10.5676(2)	13.3713(3)	10.3866(2)	23.8087(3)	12.7351(1)
c, Å	18.5330(1)	20.1485(2)	40.2425(10)	18.7774(3)	15.7753(3)	19.8068(3)	26.2516(1)	20.6397(2)
α, deg	90	90	90	76.960(1)	92.310(1)	90	64.522(1)	75.511(1)
β, deg	106.427(1)	102.507(1)	95.578(1)	76.443(1)	109.491(1)	102.103(1)	82.590(1)	82.520(1)
γ, deg	90	90	90	61.982(1)	114.119(1)	90	89.910(1)	71.545(1)
volume, Å^3	4423.41(8)	4710.53(12)	4178.50(18)	1765.94(6)	2305.04(8)	3754.39(9)	7486.61(11)	2892.38(6)
no. of reflns for unit cell determination	7021	6881	7519	5631	5364	8192	7996	7927
Z	4	4	4	2	2	4	2	2
density (calcd), g/cm^3	2.159	2.087	2.241	2.418	2.194	2.324	1.675	1.985
abs coeff, mm^{-1}	9.283	8.721	9.823	11.608	9.026	10.925	5.573	7.230
F(000)	2664	2760	2608	1176	1416	2408	3607	1636
cryst size, mm^3	0.430 × 0.390 × 0.160	0.240 × 0.220 × 0.180	0.260 × 0.120 × 0.110	0.38 × 0.38 × 0.24	0.16 × 0.10 × 0.04	0.26 × 0.10 × 0.05	0.24 × 0.14 × 0.06	0.28 × 0.15 × 0.10
θ range for data collection, deg	2.01 to 29.31	2.02 to 29.39	2.11 to 29.37	2.20 to 29.24	2.11 to 29.31	2.10 to 29.29	2.04 to 29.37	2.01 to 29.30
index ranges	$-18 \le h \le 17$, $0 \le k \le 25$, $0 \le l \le 24$	$-18 \le h \le 18$, $0 \le k \le 22$, $0 \le l \le 27$	$-12 \le h \le 12$, $0 \le k \le 14$, $0 \le l \le 52$	$-13 \le h \le 13$, $-13 \le k \le 14$, $0 \le l \le 25$	$-17 \le h \le 16$, $-18 \le k \le 18$, $0 \le l \le 21$	$-25 \le h \le 24$, $0 \le k \le 14$, $0 \le l \le 26$	$-17 \le h \le 17$, $-28 \le k \le 31$,$0 \le l \le 36$	$-15 \le h \le 16$, $-16 \le k \le 17$, $0 \le l \le 28$
no. of reflns collected	28 891	30 987	31 484	14 981	19 571	24 444	55 114	21 980
no. of ind reflns	10920 [R(int) = 0.0360]	11660 [R(int) = 0.0380]	10411 [R(int) = 0.0386]	8373 [R(int) = 0.0298]	10931 [R(int) = 0.0685]	9318 [R(int) = 0.0423]	34796 [R(int) = 0.0616]	13670 [R(int) = 0.0226]
max. and min. transmn	0.189284, 0.100457	0.297276, 0.195012	0.432052, 0.269139	0.121436, 0.057538	0.526835, 0.347287	0.461175, 0.311235	0.603987, 0.455841	0.583495, 0.321392
no. of data/restraints/ params	10 920/6/548	11 660/0/563	10 411/2/517	8373/2/427	10 931/2/562	9318/0/442	24 945/4/522	13 670/2/698
goodness-of-fit on F^2	1.149	1.074	1.251	1.125	0.967	1.132	1.039	1.186
final R indices [$I>2\sigma(I)$]	R1 = 0.0457, wR2 = 0.0986	R1 = 0.0394, wR2 = 0.0698	R1 = 0.0436, wR2 = 0.0877	R1 = 0.0352, wR2 = 0.0821	R1 = 0.0646, wR2 = 0.1130	R1 = 0.0456, wR2 = 0.0691	R1 = 0.0715, wR2 = 0.1657	R1 = 0.0330, wR2 = 0.0781
R indices (all data)	R1 = 0.0716, wR2 = 0.1110	R1 = 0.0689, wR2 = 0.0810	R1 = 0.0628, wR2 = 0.0936	R1 = 0.0425, wR2 = 0.0867	R1 = 0.1620, wR2 = 0.1472	R1 = 0.0869, wR2 = 0.0822	R1 = 0.1335, wR2 = 0.1996	R1 = 0.0443, wR2 = 0.0855
largest diff peak and hole, e Å^{-3}	1.722 and −1.572	1.374 and −1.422	0.985 and −1.868	1.377 and −2.150	2.146 and −2.461	0.765 and −1.024	2.318 and −2.334	0.960 and −1.418

minimization of steric interactions between the bulky phosphine ligands.

Concluding Remarks

We have found that the osmium−antimony cluster $Os_3(\mu\text{-}H)(\mu\text{-}SbPh_2)(\mu_3,\eta^2\text{-}C_6H_4)(CO)_9$ is very reactive, its reaction with PPh_3 proceeding even under ambient conditions to initially afford a nucleophilic addition product which can rapidly isomerize, decarbonylate, deorthometalate, or react further with excess PPh_3 to give an orthometalated product, $Os_3(\mu\text{-}SbPh_2)(CO)_8(PPh_2C_6H_4)(PPh_3)_2$. The origin of the orthometalated phenyl ring in this product has been established via the reaction of a *p*-tolyl derivative, $Os_3(\mu\text{-}H)(\mu\text{-}SbPh_2)(\mu_2,\eta^2\text{-}C_6H_4)(CO)_9\{(p\text{-tolyl})_3P\}$, with PPh_3. Many of the new clusters isolated exhibit interesting structural features and ligand bonding modes. It is therefore apparent that there is potential for much more interesting chemistry associated with this and other osmium−antimony clusters.

Experimental Section

General Procedures. All reactions and manipulations were performed under a nitrogen atmosphere by using standard Schlenk techniques. Solvents were purified, dried, distilled, and kept under nitrogen prior to use. NMR spectra were recorded on a Bruker 300 MHz NMR spectrometer in $CDCl_3$ unless otherwise stated. FTIR spectra were recorded as solutions in CH_2Cl_2 unless otherwise stated. Microanalyses were carried out by the microanalytical laboratory at the National University of Singapore. The cluster $Os_3(\mu\text{-}H)(\mu\text{-}SbPh_2)(\mu_3,\eta^2\text{-}C_6H_4)(CO)_9$, **1**, was prepared according to the published method;[7] all other reagents were from commercial sources and used as supplied.

Reaction of 1 with PPh_3. To a solution of **1** (44 mg, 0.037 mmol) in hexane (10 mL) was added PPh_3 (15 mg, 0.057 mmol). The mixture was stirred for 20 h, upon which the initial color of the solution turned from bright yellow to light yellow. The solvent was removed on the vacuum line and the residue subjected to TLC separation to give three bands. Recrystallization of the first band gave yellow crystals of $Os_3(\mu\text{-}H)(\mu\text{-}SbPh_2)(\mu_2,\eta^2\text{-}C_6H_4)(CO)_9(PPh_3)$, **2a**, and orange crystals of $Os_3(\mu\text{-}H)(\mu\text{-}SbPh_2)(\mu_3,\eta^2\text{-}C_6H_4)(CO)_8(PPh_3)$, **3a**. Further crystallization from the supernatant afforded more crystalline samples, which contained $Os_3(\mu\text{-}H)(\mu\text{-}SbPh_2)(\mu_2,\eta^2\text{-}C_6H_4)(CO)_9(PPh_3)$, **4**, an isomer of **2a**. However, **4** could not be obtained free from contamination by **2a**. Mechanical separation of the yellow crystals of **2a** from **3a** and recrystallization of it from CH_2Cl_2/hexane again gave orange crystals of **3a**. **2a** (27 mg, 50%): IR ν(CO) 2093m, 2075s, 2013vs, 1992m, 1933w cm^{-1}; ^1H NMR δ −18.41 (d, $^2J_{PH}$ = 5.8 Hz, OsHOs); $^{31}P\{^1H\}$ NMR δ 5.46 (s). Anal. Calcd for $C_{45}H_{30}O_9Os_3PSb$: C, 37.57; H, 2.09. Found: C, 37.59; H, 2.21. **3a**: IR ν(CO) 2081m, 2037s, 2011vs, 1950m cm^{-1}; ^1H NMR δ −16.40 (d, $^2J_{PH}$ = 12.4 Hz, OsHOs); $^{31}P\{^1H\}$ NMR δ 6.75 (s). Anal. Calcd for $C_{44}H_{30}O_8Os_3PSb$: C, 37.46; H, 2.12; P, 2.20. Found: C, 37.69; H, 2.29; P, 1.84. **4**: IR ν(CO) 2098m, 2071w, 2055m, 2031m, 2019s, 1979mw,br, 1952mw,br cm^{-1}; ^1H NMR δ −18.62 (d, $^2J_{PH}$ = 7.4 Hz, OsHOs); $^{31}P\{^1H\}$ NMR δ 0.13 (s).

The second band gave a very low yield of a yellow solid that has been identified as $Os_3(\mu\text{-}SbPh_2)(Ph)(CO)_9(PPh_3)$, **5a**: IR ν(CO) 2070w, 2039m, 2003m, 1990s, 1943w cm^{-1}. The third band gave a pale yellow crystalline sample of $Os_3(\mu\text{-}SbPh_2)(CO)_8(PPh_2C_6H_4)(PPh_3)_2$, **6a** (17 mg, 25%): IR ν(CO) 2053w, 2012m, 1988s, 1970s, 1943m, 1930m, 1908w cm^{-1}; $^{31}P\{^1H\}$ NMR δ 14.35 (s), 1.41 (s), −6.03(s). Anal. Calcd for $C_{74}H_{54}O_8Os_3P_3Sb$: C, 47.86; H, 2.91. Found: C, 48.02; H, 3.13. The presence of CH_2Cl_2 solvent in the crystalline sample used for the X-ray diffraction study was confirmed by ^1H NMR spectroscopy.

Reaction of 2a with PPh_3. To a hexane solution of **2a** (20 mg, 0.014 mmol) was added PPh_3 (10 mg, 0.038 mmol). The mixture was stirred overnight to give a precipitate and a light yellow supernatant. Removal of the solvent and volatile materials in vacuo followed by TLC separation with CH_2Cl_2/hexane (30:70, v/v) as eluant gave, besides unreacted starting material (5 mg), cluster **6a** (21 mg, 71%).

Reaction of 3a with PPh_3. To a CH_2Cl_2 solution of **3a** (10 mg, 0.0071 mmol) was added PPh_3 (5 mg, 0.019 mmol). The mixture was stirred at room temperature for 20 h, when the IR spectrum of the solution showed that the starting material was consumed. TLC separation of the mixture using CH_2Cl_2/hexane (30:70, v/v) gave **6a** (13 mg, 99%).

Photolysis of 2a. A hexane solution (15 mL) of **2a** (21 mg, 0.015 mmol) was photolyzed under a UV lamp (15W, 360 nm) for 1 h. The color of the solution changed from yellow to orange, and an orange solid was precipitated. TLC separation using CH_2Cl_2/hexane (20:80, v/v) as eluant afforded **3a** (19 mg, 92%).

Decomposition of 2a on Silica Gel. A dichloromethane (15 mL) solution of **2a** (25.5 mg, 0.018 mmol) was stirred together with silica gel for 2 h. The color of the supernatant changed from yellow to orange. Filtration of the solution followed by TLC separation using CH_2Cl_2/hexane (20:80, v/v) gave **3a** (24 mg, 95%).

Reaction of 1 with $(p\text{-tolyl})_3P$. To a hexane solution (15 mL) of **1** (21.6 mg, 0.018 mmol) was added $(p\text{-tolyl})_3P$ (5 mg, 0.025 mmol). A similar workup as for the PPh_3 reaction above gave two chromatographic bands. Recrystallization of the first yellow band gave yellow crystals of $Os_3(\mu\text{-}H)(\mu\text{-}SbPh_2)(\mu_2,\eta^2\text{-}C_6H_4)(CO)_9\{(p\text{-tolyl})_3P\}$, **2b** (5.3 mg, 20%), as well as orange crystals of $Os_3(\mu\text{-}H)(\mu\text{-}SbPh_2)(\mu_3,\eta^2\text{-}C_6H_4)(CO)_8\{P(p\text{-tolyl})_3\}$, **3b** (9.1 mg, 35%). Mechanical separation of **2b** and recrystallization from a CH_2Cl_2/hexane solution again afforded **3b**. **2b**: IR ν(CO) 2092m, 2073vs, 2011vs, 2007vs, 1932w cm^{-1}; ^1H NMR δ −18.60 (d, $^2J_{PH}$ = 8.3 Hz, OsHOs); $^{31}P\{^1H\}$ NMR δ −2.10 (s). Anal. Calcd for $C_{48}H_{36}O_9Os_3PSb$: C, 38.94; H, 2.43; P, 2.10. Found: C, 38.87; H, 2.65; P, 1.85. **3b**: IR ν(CO) 2080s, 2036s, 2009vs, 1957m, 1948m cm^{-1}; ^1H NMR δ −16.22 (d, $^2J_{PH}$ = 10.7 Hz, OsHOs); $^{31}P\{^1H\}$ NMR δ 3.99 (s). Anal. Calcd for $C_{47}H_{36}O_8Os_3PSb\cdot 1/4$hexane: C, 39.53; H, 2.70. Found: C, 39.29; H, 2.66. The presence of hexane was confirmed by ^1H NMR spectroscopy.

The second band gave $Os_3(\mu\text{-}SbPh_2)(CO)_8\{\mu\text{-}P(p\text{-tolyl})_2(C_6H_3CH_3)\}\{P(p\text{-tolyl})_3\}_2$, **6b** (9.3 mg, 26%): IR ν(CO) 2050w, 2008m, 1987s, 1969s, 1941m,br cm^{-1}; $^{31}P\{^1H\}$ NMR δ 12.47 (s), 0.91 (s), −8.04 (s). Anal. Calcd for $C_{83}H_{72}O_8Os_3P_3Sb$: C, 50.27; H, 3.63. Found: C, 50.52; H, 3.80.

Reaction of 2b with PPh_3. To a CH_2Cl_2 solution of **2b** (20 mg, 0.014 mmol) was added PPh_3 (10.6 mg, 0.040 mmol). The mixture was stirred overnight, whereupon the solution turned to a light yellow. TLC separation using CH_2Cl_2/hexane (30:70, v/v) as eluant gave only one product, $Os_3(\mu\text{-}SbPh_2)(CO)_8\{\mu\text{-}P(p\text{-tolyl})_2(C_6H_3CH_3)\}(PPh_3)_2$, **8** (23.6 mg, 90%): IR ν(CO) 2052w, 2011m, 1988s, 1968s, 1941m cm^{-1}; $^{31}P\{^1H\}$ NMR δ 12.28 (s), 1.63 (s), −5.71 (s). Anal. Calcd for $C_{77}H_{60}O_8Os_3P_3Sb$: C, 48.70; H, 3.16. Found: C, 48.80; H, 3.42.

Reaction of 1 with PPh_3 and TMNO. To a solution of **1** (32 mg, 0.027 mmol) in CH_2Cl_2 (15 mL) was added $Me_3NO\cdot 2H_2O$ (7 mg, 0.063 mmol), followed by PPh_3 (15 mg, 0.057 mmol). The solution turned to an orange color within 15 min. Solvent and volatiles were removed under vacuum, and TLC separation of the residue using CH_2Cl_2/hexane (20:80, v/v) as eluant gave a major orange band. Recrystallization of this orange band from CH_2Cl_2/hexane gave red blocks of the cluster $Os_3(\mu\text{-}H)(\mu\text{-}SbPh_2)(\mu_3,\eta^2\text{-}C_6H_4)(CO)_7(PPh_3)_2$, **7** (37 mg, 82%): IR ν(CO) 2070w, 2040s, 2012s, 1993m, 1966m, 1948m cm^{-1}; ^1H NMR δ −16.64 (dd, $^2J_{PH}$ = 9.1, 10.0 Hz, OsHOs); $^{31}P\{^1H\}$ NMR δ 1.60 (s), 0.75 (s). Anal. Calcd for $C_{61}H_{45}O_7Os_3P_2Sb\cdot CH_2Cl_2$:

C, 43.06; H, 2.74; P, 3.58. Found: C, 43.17; H, 2.92; P, 3.13. The presence of CH_2Cl_2 was verified by ^1H NMR spectroscopy.

Reaction of 3a with PPh_3 and TMNO. To a CH_2Cl_2 solution of **3a** (15 mg, 0.011 mmol) was added PPh_3 (5 mg, 0.019 mmol), followed by $Me_3NO{\cdot}2H_2O$ (3 mg, 0.027 mmol). The mixture was stirred at room temperature for 1 h. TLC separation using CH_2Cl_2/hexane (20:80, v/v) as eluant afforded only one product, identified by IR spectroscopy as **7** (17 mg, 98%).

Reaction of 1 with PMe_2Ph. To a solution of **1** (101.4 mg, 0.086 mmol) in hexane (10 mL) was added PMe_2Ph (13.8 mg, 0.10 mmol). The mixture was stirred at room temperature until the IR spectrum of the solution showed that **1** was consumed (15 h). Removal of the solvent followed by chromatographic separation on silica gel using dichloromethane/hexane (1:4, v/v) as eluant gave a major yellow band, from which $Os_3(\mu\text{-H})(\mu\text{-SbPh}_2)(\mu_2,\eta^2\text{-C}_6H_4)(CO)_9(PMe_2Ph)$, **2c**, was obtained (65.5 mg, 58.0%). Cluster **2c** was not stable and quickly decomposed, as shown by the change of color from yellow to orange and the change in its IR spectrum. After allowing it to stand for 1 day at room temperature, the mixture was chromatographed on silica TLC plates to give two yellow bands and an orange band. The first yellow band was found to be **2c** (10.2 mg). The second band gave yellow crystals of $Os_3(\mu\text{-H})(\mu\text{-SbPh}_2)(\mu_3,\eta^2\text{-C}_6H_4)(CO)_8(PMe_2Ph)$, **3c** (15.6 mg, 24.3%), while the third band gave orange crystals of $Os_3(\mu\text{-SbPh}_2)(Ph)(CO)_9(PMe_2Ph)$, **5c** (34.7 mg, 52.8%). **2c**: IR ν(CO) 2090w, 2073s, 2008vs,br, and 1933w,br cm^{-1}; ^1H NMR δ 7.7−7.0 (m, aromatic), 2.41 (d, $^2J_{PH} = 9.9$ Hz, P*Me*$_2$Ph), −18.88 (d, $^2J_{PH} = 7.4$ Hz, OsHOs). Anal. Calcd for $C_{35}H_{26}O_9Os_3SbP$: C, 31.99; H, 1.99. Found: C, 31.81; H, 2.22. **3c**: IR (hexane) ν(CO) 2080m, 2034s, 2011s,br, 1960w,br, and 1942m,br cm^{-1}; ^1H NMR δ 7.7−7.0 (m, aromatic), 2.41 (d, $^2J_{PH} = 10.7$ Hz, P*Me*$_2$Ph), −16.44 (d, $^2J_{PH} = 12.4$ Hz, OsHOs); $^{31}P\{^1H\}$ NMR δ −32.43 (s). Anal. Calcd for $C_{34}H_{26}O_8Os_3PSb$: C, 31.75; H, 2.04. Found: C, 31.91; H, 1.99. **5c**: IR (hexane) ν(CO) 2083w, 2036w, 2014m, 1999s, and 1942w,br cm^{-1}; ^1H NMR δ 7.6−7.2 (m, aromatic), 2.30 (d, $^2J_{PH} = 10.7$ Hz, P*Me*$_2$Ph); $^{31}P\{^1H\}$ NMR δ −31.80 (s). Anal. Calcd for $C_{35}H_{26}O_9Os_3PSb$: C, 31.99; H, 1.99. Found: C, 31.94; H, 1.88.

Crystal Structure Determination of 2a, 2b, 3a, 3c, 4, 5c, 6a, and 7. The crystals were mounted on quartz fibers. Crystal data and structure refinement details are given in Table 3. The data were measured on a Bruker APEX AXS diffractometer, equipped with a CCD detector, using Mo Kα radiation ($\lambda = 0.71073$ Å), at 293(2) K. The data were corrected for absorption effects with SADABS.[18] The final unit cell parameters were obtained by least squares on a number of strong reflections. Structural solution and refinement were carried out with the SHELXTL suite of programs.[19] The structure was solved by direct methods to locate the heavy atoms, followed by difference maps for the light, non-hydrogen atoms. The phenyl hydrogens were placed in calculated positions. Metal hydride positions were calculated with XHYDEX[20] (except for **2b**, in which the hydrides were located in the difference map) and allowed to ride on one of the osmium atoms that they are attached to, and given a fixed isotropic thermal parameter. All non-hydrogen atoms were given anisotropic displacement parameters in the final refinement, except for **6a** (see below).

Compound **2a** exhibited large residues close to the heavy atoms in the difference map; this was interpreted as disorder of the metal core. Thus the metal atom positions were modeled with two alternative sites. Appropriate restraints were placed on the occupancies, anisotropic thermal parameters, and the Os−Os and Os−Sb distances. Compound **6a** had two molecules in the asymmetric unit. The phenyl rings (but not the phenylenes) were regularized. All the carbon atoms were given isotropic thermal parameters; all phenyl carbon atoms were given one common thermal parameter. Two partial molecules of dichloromethane were found, and they were given occupancies of 0.5 and 0.25, the chlorine and carbon atoms were given fixed isotropic thermal paramters, and restraints were placed on the C−Cl distances.

Acknowledgment. This work was supported by the National University of Singapore (Research Grant No. RP 982751), and two of us (G.C. and M.D.) thank the University for a Research Scholarship.

Supporting Information Available: Experimental and refinement details for the crystallographic studies, tables of crystal data and structure refinement, atomic coordinates, isotropic and anisotropic thermal parameters, complete bond parameters, and hydrogen coordinates. Crystallographic data in CIF format. This material is available free of charge via the Internet at http://pubs.acs.org.

OM010959A

(18) Sheldrick, G. M. *SADABS*; University of Göttingen, 1996.
(19) *SHELXTL*, version 5.03; Siemens Energy and Automation Inc.: Madison, WI, 1995.
(20) Orpen, A. G. *XHYDEX: A Program for Locating Hydrides in Metal Complexes*; School of Chemistry, University of Bristol, UK, 1997.